Journal of Environmental Chemical Engineering 4 (2016) 3205–3216

Contents lists available at ScienceDirect

Journal of Environmental Chemical Engineering

journal homepage: www.elsevier.com/locate/jece

# An approach for the reuse of *Dacryodes edulis* leaf: Characterization, acetylation and crude oil sorption studies

Nnaemeka J.N. Nnaji[a,*], Thereasa U. Onuegbu[b], Obiageli Edokwe[b], Godwin C. Ezeh[c], Adaeze P. Ngwu[d]

[a] Department of Chemistry/Biochemistry/Molecular Biology, Federal University Ndufu Alike Ikwo, Ebonyi, Nigeria
[b] Department of Pure and Industrial Chemistry, Nnamdi Azikiwe University, Anambra, Nigeria
[c] Center for Energy Research Development, Obafemi Awolowo University, Osun, Nigeria
[d] Department of Industrial Chemistry, Caritas University, Enugu, Nigeria

ARTICLE INFO

*Article history:*
Received 1 March 2016
Received in revised form 5 June 2016
Accepted 8 June 2016
Available online 2 July 2016

*Keywords:*
Dacryodes edulis leaf
Acetylation
Crude oil sorption

ABSTRACT

This work investigated the modification of Dacyodes edulis leaf (DEL) by acetylation to give acetylated Dacryodes edulis leaf (ADEL) and their applications to treatment of crude oil polluted waters. DEL acetylation was favoured by low temperature, increased time of acetylation, and in the absence of catalyst. Crude oil sorption kinetic data were best fitted by liquid film diffusion and pseudo-first order kinetic models for DEL, but pseudo-second order kinetic model best fits crude oil sorption data by ADEL. Equilibrium crude oil sorption data were best fitted into Langmuir and Freundlich isotherms for ADEL and DEL respectively. Results suggest that ADEL is more suitable for crude oil sorption than DEL, therefore, possesses more potential for application in treatment of oil spillage.



## 1. Introduction

Crude oil exploration is an important activity of man considering that it is a major source of energy for vehicular, domestic and industrial activities. Consequently, crude oil explorations often cause spills that result in pollutions of affected sea and land regions. Aquatic lives, vegetation and man have suffered severely from crude oil pollutions there is therefore the need to direct recent research towards discovering efficient materials for clean-up of crude oil polluted waters (COPOWs). However, materials which are biodegradable, cheap, environmentaly friendly and readily available make this area of scholasticism challenging. Interestingly, the use of agricultural by-products meet these required attributes, therefore, they are reportedly in vogue for applications in clean-up of COPOWs [1–3]. Chemical modification, by acetylation, of agricultural byproducts have been reported to enhance the effectiveness of the materials by decreasing the density of the hydroxyl functionality [4]. Examples of acetylated materials used for crude oil sorption studies include: corncobs, rice husks, banana fibre [2,3,5] and kapok fiber for gasoline oil [6]

Plants are important in our everyday existence. They provide our foods, produce the oxygen we breathe, and serve as raw materials for many industrial products such as clothes, foot wears and so many others. Plants also provide raw materials for our buildings and in the manufacture of biofuels, dyes, perfumes, pesticides, adsorbents and drugs. *Dacryodes edulis*, however, is an odiferous fruit tree found in equatorial and humid tropic climates and originates from Central Africa and Gulf of Guinea area [7]. Much work has been done on *Dacryodes edulis*. For example, Ikhuoria and Maliki [8] characterized the oil from *Dacryodes edulis* pear, Okwu and Nnamdi [9] investigated the phytochemical contents and medicinal values of *Dacryodes edulis* exudates. The inhibitive effect of exudate gum from *Dacroydes edulis* on the acid corrosion of aluminium was studied by Umoren and co-workers [10]. Also, Oguzie et al. [11] studied DEL extract as an alternative steel corrosion inhibitor. However, there appears not to be any work(s) on the application(s) of *Dacryodes edulis* leaf (DEL) in crude oil polluted water.

Classes of oil sorbents may include organic synthetic [12], inorganic mineral and agro-based products [13]. Notably, many organic synthetic products such as polypropylene and polyurethane, used as commercial oil sorbents present challenges because they are relatively expensive [14] and pose disposal problems due their xenobiotic nature [15]. Teas et al. [16] reported perlite, graphite, clay and so on as examples of inorganic mineral oil

* Corresponding author.
*E-mail address:* joemeks4u@yahoo.com (N.J.N. Nnaji).

http://dx.doi.org/10.1016/j.jece.2016.06.010
2213-3437/

sorbents which possess environmental disposal challenges caused by slow degradation [16]. Agro-based products are the class of sorbents which now attract great interest because of their improved properties over the organic synthetic and inorganic mineral sorbents. Amongst these properties are: good oil absorbency, ready availability, inexpensive and cost savings in disposal fee [15]. Consequently, studies on some agro-based oil sorbents such as kapok, milkweed and cotton, were carried out and results suggest that they possess good oil sorption properties [15,17].

On one part, the purpose of this work is to assess the physico-chemical properties of Dacryodes edulis leaf (DEL) for its use as an environmental clean-up raw material for crude oil polluted water. On another part, the modification of DEL by acetylation, the mechanism and thermodynamics of the process were monitored in detail. Also, detailed kinetic and equilibrium studies of crude oil and water sorptions by DEL and ADEL were done.

## 2. Materials and methods

### 2.1. Material preparation

DEL was sourced locally from beneath trees near the University of Nigeria Nsukka campus. Thorough washing was done with water and properly air dried (during harmattan). They were size reduced and sieved through 20 and 25 British Standard Sieve (BSS Sieves) so that particle sizes in the range $707 - 841\mu\mu$ were used. Reagents and chemicals, of analytical grades, used were from British Drug House (BDH) and include acetic anhydride, N-Bromosuccinimide (NBS), Acetone, Ethanol and *n*-Hexane, and were used without further purification.

The sieved material (100 g) was extracted with a mixture of acetone and *n*-hexane ($4:1\frac{v}{v}$) for 5 h (to reduce the influence of the fibre extractibles on acetylation), dried in a laboratory oven (operated in the range of 60–70 °C) for 16 h and stored in a desiccator at room temperature thereafter. The extractible content was calculated on a percentage of the oven-dried test samples.

### 2.2. Methods

#### 2.2.1. Characterisation of DEL

*2.2.1.1. Density determinations.* 20 g of the sample was used to fill up a container of 100 mL volume and the bulk density was then calculated using the following expression [18]:

$$\text{Bulk density} = \frac{w}{v} \tag{1}$$

where w is weight of the sample and v is volume of the container.

After two hundred 'taps, mechanically, a new volume ($v_{200}$) was obtained. The mechanical tapping was performed by raising the cylinder and allowing it to drop through a safe height, under its own mass. Tapped density was calculated using the following expression

$$\text{Tapped density} = \frac{w}{v_{200}} \tag{2}$$

where w is weight of the sample and $v_{200}$ is 'tapped' volume of the container.

As described by Ejikeme [18], true density was determined by the liquid displacement method using xylene as the immersion fluid. True density was calculated using the following expression

$$\text{Time density} = \frac{w}{v_T} \tag{3}$$

where w is weight of the sample and $v_T$ is 'true volume of the container.

*2.2.1.2. Determination of percentage ash content.* 2.0 g of the sample was weighed into a pre-weighed crucible and burnt over a Bunsen burner flame until there was no more smoke. The sample was then placed in the muffle furnace at 600 °C until it turned grey-white. This was cooled in a dessicator and weighed to a constant weight. The following expression was used to calculate ash content [19]:

$$\text{Ash content}(\%) = \frac{w_{ash}}{w_{sample}} \times 100 \tag{4}$$

where $w_{ash}$ is weight of ash and $w_{sample}$ is weight of sample.

*2.2.1.3. Percentage moisture content.* 2 g of the ground sample was weighed into a pre-weighed crucible. The crucible and the content were weighed again. This was then put in the oven at 101 °C for 2 h after which it was removed, cooled and weighed until a constant weight was obtained. The expression used to calculate the moisture content is [19]:

$$\text{Moisture content}(\%) = \frac{w_{sample} - w_{dry}}{w_{sample}} \times 100 \tag{5}$$

where $w_{sample}$ is the weight of sample before drying, $w_{dry}$ is weight of sample after drying.

*2.2.1.4. Determinations of cellulose, hemicellulose and lignin.* Compositions of cellulose, hemicellulose and lignin in DEL were determined as described elsewhere [5].

#### 2.2.2. Determination of mineral composition

Available XRF equipment is portable AMPTEK(R) for Energy Dispersive X-ray Fluorescence (EDXRF) measurements. Sample preparation was done by pulverizing the sample to fine powdery form using an agate mortar and a pellet of the sample was formed using a CARVER model manual pelletizing machine at a pressure of 6-8 Torr. The pelletized sample was inserted into the sample holder of the XRF system and was bombarded by X-ray fluorescence spectrometer with a Ag anode at a voltage of 25 kV and current of 50 μA for 1000 counts or approximately 18 min in an external chamber setup. The equipment model is PX 2CR Power Supply and Amplifier for XR-100CR Si-pin Detector. Characteristic X-ray of the sample was detected by the solid state Si-Li detector system and spectrum acquisition was done using ADMCA[R]software. The spectrum analysis was done using the ADMCA plus Fundamental Parameter (FP-CROSS) software which translates the peak areas into concentration values.

#### 2.2.3. Acetylation of DEL

The method of Nwadiogbu et al. [2] was adopted for DEL acetylation as briefly described. The combination ratio during acetylation was in a ratio of 1:20 ($^{w}/_{v}$ of DEL: acetic anhydride). Respectively, the reaction temperature, time and amount of catalyst (NBS) were varied from 30 °C to 100 °C, 1 h to 3 h and 0–4%. After acetylation, DEL was thoroughly washed with ethanol and acetone to remove unreacted acetic anhydride and acetic acid (as by-product). The new product, acetylated dacryodes edulis leaf (ADEL), was dried in an oven at 60 °C for 16 h prior to analysis. The extent of acetylation was determined from the infrared spectra of ADEL samples by calculating the ratio of the intensity of the acetyl C=O band (around 1740–1745 $cm^{-1}$) to the intensity of the C—O signals of cellulose (at about 1020–1040 $cm^{-1}$) [20]:

$$R = \frac{I_{1740}}{I_{1020}} \tag{6}$$

The effects of three factors, namely: (i) temperature, (ii) time and (iii) catalyst, on acetylation were investigated and the data were statistically analysed for significance using SPSS version 21.

*2.2.4. Sorption capacity studies*

DEL and ADEL samples, 1 g each, were allowed to absorb water at 5–120 min time intervals. Afterwards, the water loaded samples were drained on the filter paper for ten minutes under vacuum filtration. The water absorption capacity (g/g) was calculated using Eq. (7):

$$\text{Water absorption capacity}(Q_w) = \frac{S_{wet} - S_{dry}}{S_{dry}} \quad (7)$$

where AW stands for amount of wet sorbent and AD stands for amount of dry sorbent.

2 g of sorbent (DEL or ADEL) was put in a 250 mL beaker containing 100 mL (87 g) of crude oil at 30 °C. With small agitations on a mechanical shaker, this was allowed to stand for 120 min. The sorbents were removed from the beakers using sieve nets and the nets were allowed to drain-off the excess oil. Afterwards, the oil-loaded sorbents were re-weighed and the crude oil sorption capacity (absorbency) was calculated using Eq. (8):

$$\text{Absorbency}(q) = \frac{S_{oil} - S_i}{S_i} \quad (8)$$

where $S_i$ is the initial weight of the dry sorbent, $S_{oil}$ is the weight of the sorbent with crude oil.

Adsorption kinetic experiments were done at 30 °C on a mechanical shaker using 250 mL beakers containing 100 mL (87 g) of crude oil and 2 g of sorbent at 5–120 min intervals. The sorption capacity of the sorbents at different time intervals were calculated using Eq. (9) [21]:

$$\text{Adsorption capacity} q_t = \frac{(C_0 - C_t)v}{m} \quad (9)$$

where $C_0$ and $C_t$ are respectively initial crude oil concentration and crude oil concentrations after different adsorption times in mg/L uints, m (g) is the mass of the sorbent and v is the volume of crude oil in L unit.

Equilibrium adsorption experiments were done at 30 °C on a mechanical shaker using 250 mL beakers containing 500–1300 g/L of crude oil and 2 g of sorbent (DEL and ADEL) for 120 min. The sorbents were removed from the beakers using sieve nets and the nets were allowed to drain. The crude oil equilibrium sorption capacity (g/g) was calculated using Eq. (10) [22]:

$$\text{Adsorption capacity}(q_e) = \frac{(C_0 - C_e)v}{m} \quad (10)$$

where $C_0$ and $C_e$ are the initial and the equilibrium crude oil concentrations (g/L) respectively, v is the volume of dye solution used (L) and m is the weight of the sorbent (g).

*2.3. Some physical properties of the crude oils*

Specific gravity bottles were used to determine the crude oil density. Ferranti portable viscometer was used to measure the crude oil viscosity, in poise, and converted to $mm^2/s$.

## 3. Results and discussion

*3.1. Characterisation*

The proximate composition of DEL is given in Table 1. Our results show that the moisture content (3.96%) is very low compared to the value of 89.00% obtained and reported by Okaraonye and Ikewuchi [23] for Penniselum purpureum.

**Table 1**
Proximate analyses on African pear leaf.

| Parameter | Value |
|---|---|
| Ash (%) | 12.881 |
| Moisture (%) | 3.960 |
| Cellulose (%) | 43.400 |
| Hemicellulose (%) | 28.270 |
| Lignin (%) | 19.000 |
| Bulk density (g/cm$^3$) | 0.296 |
| Tapped density (g/cm$^3$) | 0.315 |
| True density (g/cm$^3$) | 1.075 |
| Carr's index | 6.032 |
| Porosity (%) | 70.698 |
| Hausner Index | 1.064 |

Considering the moisture content of any food is an index of its water activity [24], it is used as a measure of stability and the susceptibility of microbial contamination [25]. This implies that DEL will very likely have a long shelf life low microbial contamination level because of its low moisture content.

Ash content value is 12.881%, higher when compared with levels found in other leaves- A. africana (4.03%) and R. glabra (4.34%). DEL ash content indicates it contains good level of mineral contents because low ash content suggests low mineral composition [26,27].

Table 1 presents density values as follows: 0.296 gcm$^{-3}$ (bulk), 0.315 gcm$^{-3}$ (tapped) and 1.075 gcm$^{-3}$ (true). Compared to 1.5 gcm$^{-3}$, 1.3 gcm$^{-3}$ and 1.2 gcm$^{-3}$ respectively for flax, jute and coir [28], value of 1.075 gcm$^{-3}$ is lower. Reported value of bulk density for corncob is 0.293 gcm$^{-3}$ [29] and is lower than 0.296 gcm$^{-3}$ for DEL. Lower bulk density has been shown to improve sorption properties of sorbents due to increased internal surfaces [30]. The value of tapped density is 0.327 gcm$^{-3}$ for corncob and is higher for DEL.

Higher tapped density values consequently are known to cause materials to be more porous. Evidently, porosity value of 81.5% is reported for corncob and is higher than 70.698% for DEL. Ejikeme [18] reported that porosity of a material is made up of voids between the particles and the pores within the particles. Arguably, this suggests that more porous materials possess better sorption properties. Table 1 presents good porosity value for DEL.

The yield of cellulose was 43.4%, higher than the yield for untreated rice husks (35.0%) [31]. Cellulose is a polymeric component that enhances the hydrophilicity of lignocellulosic materials due to presence of poly-hydroxyl groups. Its yield suggests it is a significant composition of DEL and supported by SEM result presented in Fig. 2a. Hydrophilic properties of lignocellulosic materials can be reduced by substitutions of acetyl groups for the poly-hydroxyl groups, often to improve the hydrophobic properties of the (modified) materials [2].

Lignin is present in DEL, 19.0% as shown in Table 1. This value is lower than that of corn cob ($16.50 \pm 2.00\%$). However, this contrasts for hemicellulose contents: 28.27% (DEL) lower than $43.1 \pm 4.00\%$ (corn cob) [32].

Table 2 presents results of the mineral compositions of DEL. The results reveal the presence of transition metals such as Fe, Cr, Mn, Cu, Ni, and the likes. Transition metals are known to complex with water molecule, as such, their presence seem to be responsible for the hydrophilic properties of materials. This is in agreement with findings elsewhere [29]. Iron deficiency is common in areas where high burden of malaria and invasive non-typhoid *Salmonella* diseases exist, therefore, it is recommended to restrict iron supplementation to people with iron deficiency [33]. Zinc is required for normal immune function because it reduces the incidence of diarrhea and pneumonia, and is essential for a variety of lymphocyte functions implicated in malaria resistance [34]. While blood calcium imbalance leads to tetany and convulsions,

**Table 2**
Mineral composition of DEL.

| Parameter | Concentration Value DEL | Unit |
|---|---|---|
| K | 975 ± 47 | ppm |
| Ca | 4070 ± 96 | ppm |
| Ti | 160 ± 19 | ppm |
| Cr | 126 ± 20 | ppm |
| Mn | 379 ± 38 | ppm |
| Fe | 1.9027 ± 0.0288 | % |
| Ni | 859 ± 65 | ppm |
| Cu | 1792 ± 101 | ppm |
| Zn | 1577 ± 102 | ppm |
| Rb | 1580 ± 168 | ppm |
| V | 127 ± 19 | ppm |
| Se | 890 ± 101 | ppm |
| Co | 391 ± 44 | ppm |
| Mo | 1221 ± 207 | ppm |

potassium is the principal cation in intracellular fluid which aid conductions of nerve impulses and muscle contractions, and copper is an essential micro-nutrient necessary for the haematologic and neurologic systems [35]. Selenium is a constituent element of the entire defence system that protects the living organism from harmful action of free radicals [35]. Brief highlights of some elements suggest that DEL is an important source of these metals. Except for potassium that has lowest content, calcium, iron, manganese and zinc have highest contents in DEL than values reported for cabbage, pumpkin and water leaves [36].

### 3.1.1. Physical properties of crude oil

The crude oil sample, Bonny Export, has 33.8$^0$ ($^0$API gravity) value suggesting it is a heavy crude. Its (kinematic) viscosity value is 6.99 mm$^2$/s and has a density of 0.868 $^g$/cm$^3$. Values of measured physical properties of the crude oil sample suggest it possesses intermediate viscosity, is less volatile and has good compositional uniformity, therefore, translates the crude oil most likely had stable physico-chemical properties during experiments [15,37].

### 3.2. Effects of acetylation on DEL

Fig. 1a and b present infrared spectra of DEL and acetylated *Dacryodes edulis* leaf (ADEL) respectively. Fig. 1a and b present prominent absorption peaks and assignments are consistent with

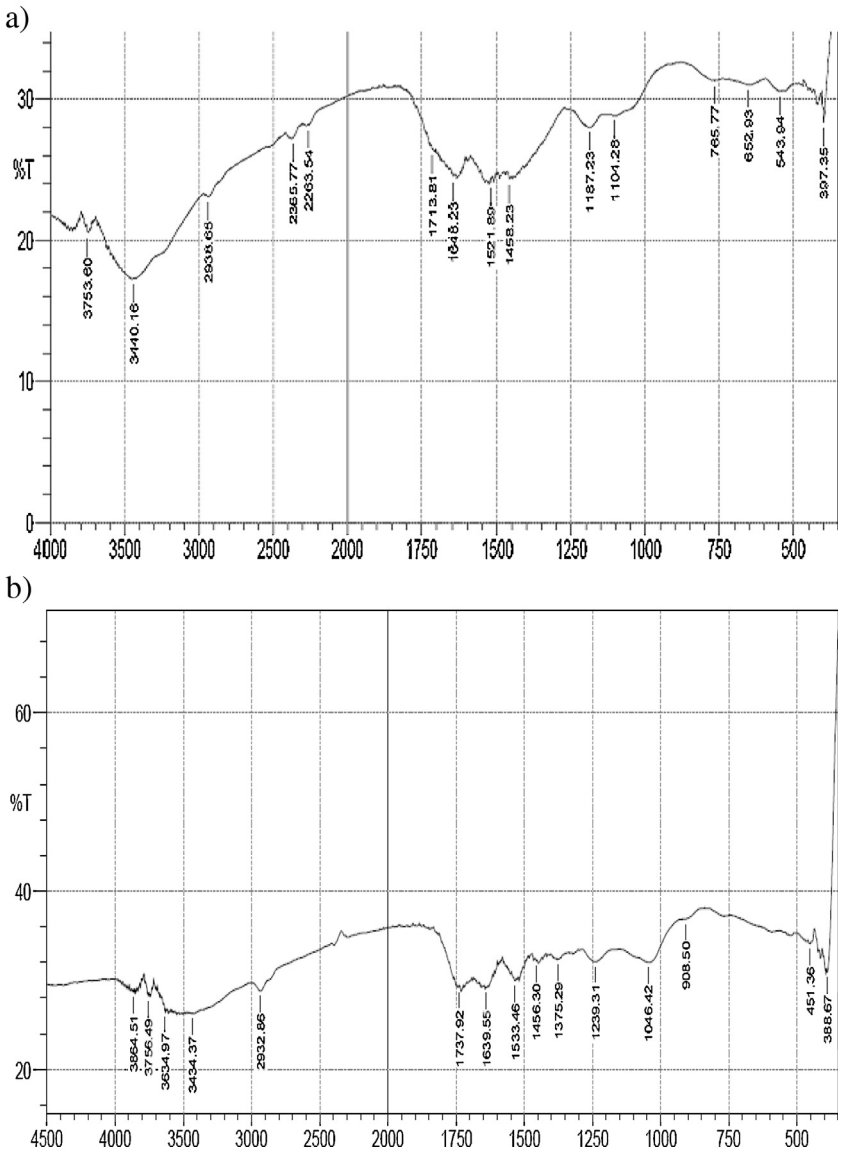


**Fig. 1.** FTIR spectra of: (a) DEL and (b) ADEL.

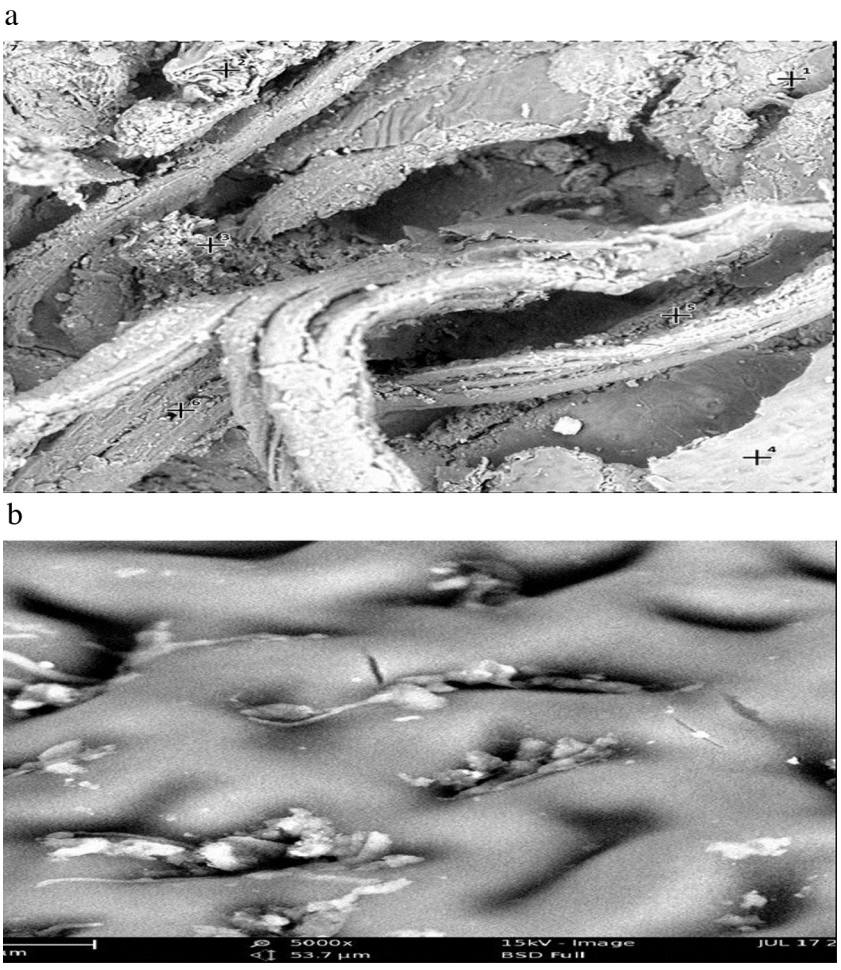


**Fig. 2.** SEM of (a) DEL and (b) ADEL.

reports elsewhere [2,4,14,38–44]. Vibrational signals within 3000–3600 $cm^{-1}$ are for −OH streching vibrations [38–40]. Signals in the range 1600–1800 $cm^{-1}$ are due to C=O stretching vibrations [41]. Vibrations seen within 1100–1300 $cm^{-1}$ are characteristic of C-O stretching signals of carboxylic, esters and ethers [41]. Broad absorption, due to O-H signal, with center at 3440 $cm^{-1}$ for DEL shifted to 3434 $cm^{-1}$ for ADEL suggesting that polyhydroxyl functional groups of DEL were involved in the acetylation process. Similar results for −OH signals in the regions were proposed for −OH vibrations of untreated kapok fibre [40] and bio-oils [41]. In addition, Figs. 1a and 1b show remarkable change in intensity (presented as% transmitance) strongly supporting efficient acetylation of DEL. Earlier, findings reported for corn cob [2], cotton [14] and sugarcane bagasse [42] are in excellent agreement with presented results that change in absorption intensity suggests effective acetylation. The implication is that some acetyl functional groups (from acetic anhydride) effectively attached to the DEL by replacing the hydroxyl groups. Before acetylation, absorption peak at 1648 $cm^{-1}$ for DEL was seen, as Fig. 1a shows, but this signal shifted to 1640 $cm^{-1}$ and suggests the presence of hemicellulose [2]. A new peak appeared at 1738 $cm^{-1}$ for ADEL, due to hemicellulose [43], supports the presence of (new) ester groups, due to DEL acetylation. Similar assignment was reported by [41]. Stretching signals of C=O attached to lignin [44] are seen around 1522 $cm^{-1}$ and 1458 $cm^{-1}$ (DEL) but shifted to 1533 $cm^{-1}$ and 1456 $cm^{-1}$ respectively after acetylation. Absorption at 1239 $cm^{-1}$, for ADEL, can be ascribed to signals of C=O of lignin and infrared spectrum of DEL (Fig. 1a) did not show this signal. This gives further insight that reduction in cellulose content of DEL, due to acetylation, caused the signal of lignin to appear for ADEL (shown in Fig. 1b). A peak at 1048 $cm^{-1}$, in Fig. 1b and ascribed to the presence of cellulose and hemicellulose [2,45], is for C—O absorption and suggests the effective acetylation of DEL to ADEL as proposed in Scheme 1 below:

Fig. 2a presents the surface of DEL suggesting/revealing its rough. After acetylation, Fig. 2b presents a distinct change in the surface morphology of DEL supporting it was effectively acetylated to ADEL. This surface change seems smooth and thick, and most likely explains the hydrophobicity of the surface after acetylation. The thickened structure shown in Fig. 2b suggests that after acetylation, DEL became bulkier due to attachments of acetyl groups (which are heavier than the hydroxyl groups), as such the area of the internal surfaces will decrease after acetylation. Surface area is a factor known to affect rate of a reaction such that smaller particles possess larger exposed or assessed surfaces than larger particles which possess smaller assessed surfaces. Arguably, ADEL

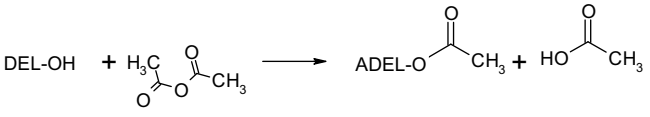


**Scheme 1.** Proposed DEL acetylation mechanism.

particles have smaller surfaces for easier assess than DEL particles, hence, the surface area required for crude oil sorption possessed by ADEL particles are larger than those of DEL.

The elemental composition of DEL before (Fig. 3a) and after (Fig. 3b) acetylation by energy dispersive X-ray (coupled with SEM measurements) reveals a reduction in oxygen availability as evidenced by the decrease in peak height of oxygen signal. This accounts for the successful replacements of −OH groups by acetyl groups (by acetylation). EDX results support results from infrared spectroscopy, in that, effective DEL acetylation was due to efficient replacements of hydrophilic hydroxyl groups of cellulose by the hydrophobic acetyl groups of the acetic anhydride. Similar results are reported elsewhere [5].

Fig. 4 presents the effects of time and temperature on DEL acetylation. The trends observed in Fig. 4 are such that the extent of acetylation: was highest after three hours at all temperatures; and was highest for most varied time intervals at 30 °C. In agreement with this study, other works have demonstrated negative temperature [46] and positive time [47] effects on acetylation of agro-materials.

The effects of time, catalyst and temperature on extent of DEL acetylation were tested for statistical difference and presented on Table 3. The results show that increasing time of acetylation has significant positive effects on extent of DEL acetylation. The effects of catalyst and temperature had negative effects.

The quantitative contributions of catalyst, time and temperature on extent of acetylation were determined using linear regression and gives the following expression (at 95% confidence).

$$EA = 0.939 - 0.003Cat - 0.008Temp + 0.011Time \quad (11)$$

EA represents extent of acetylation, Time means acetylation time, Temp stands for temperature and Cat means catalyst. Eq. (11) suggests that: 0.8% percent decrease in EA was due to 1 ° rise in temperature (in K), 0.3% percent decrease in EA was due to 1% g/mL increase in quantity of catalyst, and 1.1% increase in EA was due to an increase in time by one minute. Eq. (10) supports that effects of catalyst and temperature on extent of acetylation are negative but time effect was positive.

### 3.3. Kinetics of DEL acetylation

The kinetics of DEL was studied by fitting obtained data in the intra-particle diffusion rate curve. This is because reports [2,48] have shown that acetylation kinetics of materials is well accounted for by the intra-particle diffusion model.

Equation representing intra-particle diffusion is [49]:

$$q_t = k_i\sqrt{t} + c \quad (12)$$

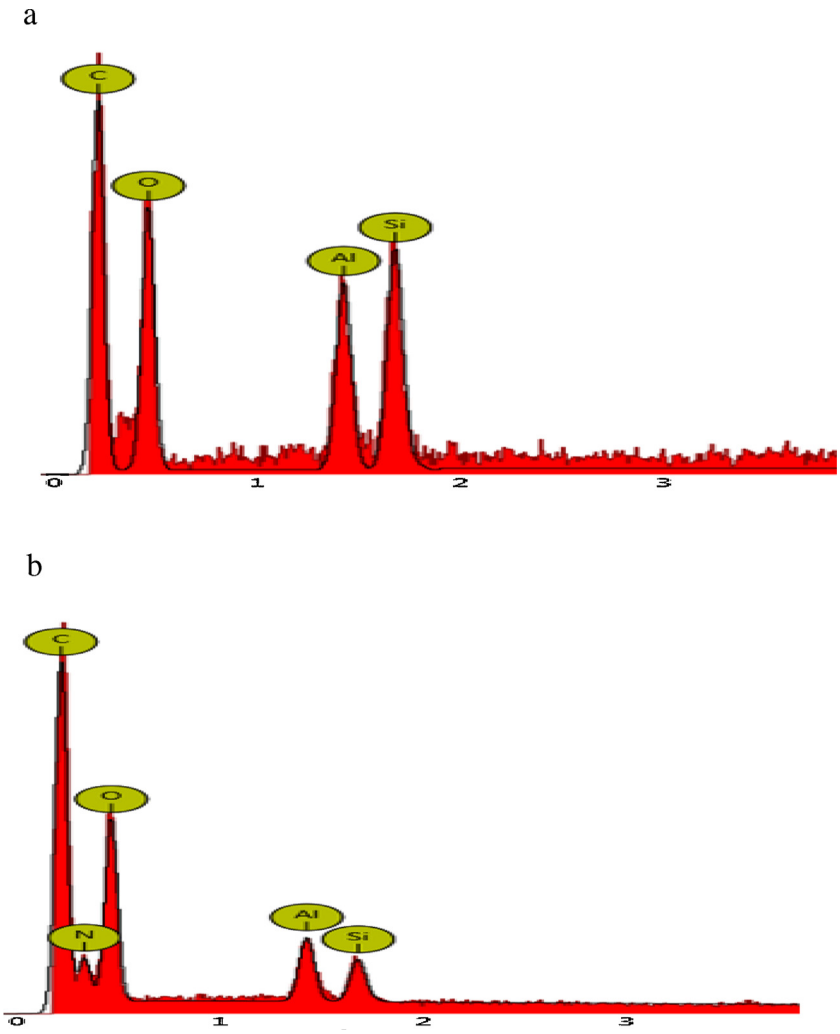


**Fig. 3.** EDX of (a) DEL; (b) ADEL.

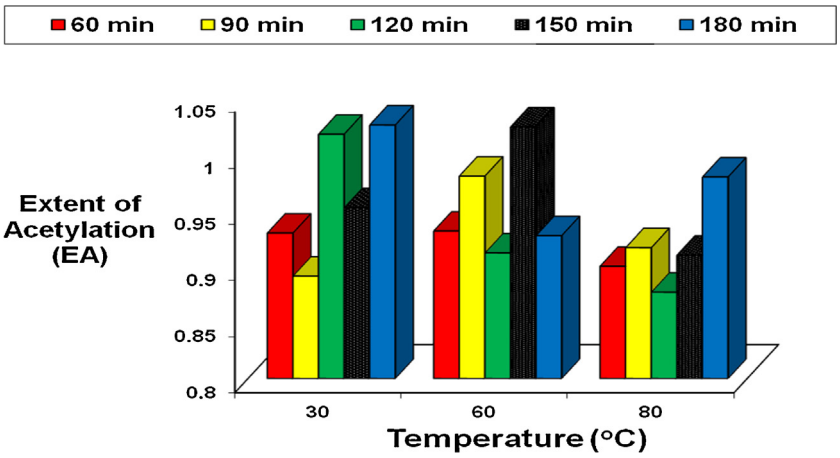


**Fig. 4.** Effects of time and temperature on extent of DEL acetylation.

Plots of Eq. (12) were performed and the following equations obtained:

at 353 Kel:

$$Y = 0.0152X + 0.8708,\ R^2 = 0.3962 \quad (13)$$

at 333 Kel:

$$Y = 0.0036X + 0.9442,\ R^2 = 0.0147 \quad (14)$$

at 303 Kel:

$$Y = 0254X + 0.8871,\ R^2 = 0.4829. \quad (15)$$

The coefficient of linearity values are less than 50% (that is $\leq$0.5), similar with result obtained elsewhere [2]. Values within $0.43 \leq R^2 \leq 0.83$ are moderate and high [50], therefore, acetylation profile at 303 Kel is good because coefficient of linearity value ($R^2$) is 0.4829 at 303 Kel. This supports negative effect of temperature on DEL acetylation.

It is expected that the plot of $q_t$ versus $t^{1/2}$ would give linear relationship when intraparticle diffusion is involved in the acetylation processes and that intraparticle diffusion would be the controlling mechanism if the line passed through the origin [49]. However for the case where the plots do not pass through the origin, the reason has been suggested that the intraparticle diffusion is not the only mechanism involved in the acetylation process due to some degree of boundary layer control [51]. Therefore, values of intercept in Eqs. (12)–(14) suggest surface reaction and intra-particle diffusion kinetics of DEL acetylation. This is in agreement with results elsewhere [2,48].

### 3.4. Thermodynamics of DEL acetylation

The thermodynamics of DEL acetylation was studied using the following equation:

$$\frac{d\ln[EA]}{dT} = \frac{\Delta H}{RT^2} \quad (16)$$

**Table 3**
Extent of DEL acetylation-correlation effects (at 95% confidence level).

| | Pearson Correlation | | | |
|---|---|---|---|---|
| | EA | Catalyst | Temperature | Time |
| EA | 1.000 | | | |
| Catalyst | −0.207 | 1.000 | | |
| Temperature | −0.377 | 0.262 | 1.000 | |
| Time | 0.438 | −0.28 | −0.341 | 1.0001 |

Eq. (16) is equivalent/similar to the Gibbs-Helmholtz equation. Integrating Eq. (16) gives the following equation below

$$\int_{[EA]_0}^{[EA]_T} \ln[EA] = \frac{\Delta H}{R}\int_{T_0}^{T}\frac{1}{T^2}dT \quad (17)$$

Solving Eq. (17) gives

$$\ln[EA]_T = -\frac{\Delta H}{RT} + \frac{\Delta H}{RT_0} + \ln[EA]_0 \quad (18)$$

Eq. (18) allows the plot of $\ln[EA]_T$ versus $T^{-1}$ where $-\frac{\Delta H}{R}$ is the slope, B represents the intercept on Y-axis ($\ln[EA]_0$), and A is the intercept on X-axis ($\frac{\Delta H}{RT_0}$). $\Delta H$ is the heat of DEL acetylation, $T_0$ is the critical temperature of acetylation (above which DEL acetylation is not favourable), and $[EA]_0$ is the critical degree of DEL acetylation.

Eq. (19) presents the obtained expression for plot using Eq. (17)

$$Y = 0.023X - 0.0669. \quad (19)$$

Acetylation of DEL was assumed to be an equilibrium surface reaction. From Eq. (19), value of slope allowed the calculation of heat of DEL acetylation to be $-0.1921\ J\,mol^{-1}$. This values suggests that DEL acetylation is an exothermic process. This explains why DEL acetylation at higher temperatures gave lower values of extent of acetylation.

The critical temperature of acetylation and critical degree of acetylation values were calculated as 303 K and 0.9325 respectively. The critical degree of DEL acetylation represents values when obtained, explains the condition of DEL acetylation. Nwadiogbu et al. [2] suggested that values above the critical degree of acetylation imply diffusion mechanism and values below it suggest surface adsorption mechanism.

The heat capacity ($C_p$) of DEL acetylation at constant pressure can be obtained using

$$\Delta H = \int_{T_1}^{T_2} C_p dT = C_p(T_2 - T_1) \quad (20)$$

$C_p$ represents the quantity of heat needed to acetylate DEL whenever a degree rise in temperature occurs. Value of $C_p$ obtained was $-3.842 \times 10^{-3}\ J\,mol^{-1}\,K^{-1}$. The negative value obtained, suggests that increasing temperature was unfavourable to DEL acetylation. The change in entropy of acetylation ($\Delta S$) was

calculated using the following equation:

$$\Delta S = C_p \ln\left(\frac{T_2}{T_1}\right) + R\ln\left(\frac{P_1}{P_2}\right) \quad (21)$$

Eq. (21) has a second term (in the right-hand side of the equation) which vanishes because the process was performed at the same pressure conditions. Therefore at the studied temperature conditions, value of change in entropy of DEL acetylation obtained is $-5.8681 \times 10^{-4}$ Jmol$^{-1}$ K$^{-1}$. The value of $\Delta S$ is negative and suggests a degree of orderliness during the acetylation processes. It can be recalled that DEL acetylation involves the reaction of acetic anhydride with the −OH sites on the material. Therefore, the replacements of these (smaller) moities with acetyl (heavier) groups to give the acetylated DEL material accounts for the orderliness process.

The Gibb's free energy is an important thermodynamic parameter, that can be calculated using

$$\Delta G = \Delta H - T\Delta S \quad (22)$$

At the studied temperature conditions, values of $\Delta G$ calculated become $-0.0143$ J mol$^{-1}$ (303 K), $-0.0055$ J mol$^{-1}$ (318 K), 0.0033 J mol$^{-1}$ (333 K), 0.0150 J mol$^{-1}$ (353 K) and 0.0268 J mol$^{-1}$ (373 K). The values are negative at lower temperatures and positive at higher temperatures. These suggest that at lower temperatures, DEL acetylation was spontaneous and favourable. However at higher temperatures, DEL acetylation was spontaneous due to the porous nature of DEL but difficult, hence, unfavourable/less efficient.

### 3.5. Water and crude oil sorption capacities

DEL and ADEL were subjected to water sorption tests. Studying DEL acetylation was majorly to observe if the modification of DEL (by acetylation) can alter its water absorption capacity, as this increases the hydrophobic properties. Fig. 5 presents the results on water absorption capacity for DEL and ADEL. Fig. 5 reveals that the water absorption capacity of DEL, about 1.97 $^{g}/_{g}$ at 120 min, is higher than the value for ADEL, 1.49 $^{g}/_{g}$ at 120 min. Fig. 5 also shows that the water absorption capacity of DEL was higher, at all times, than for ADEL. Replacements of the poly-hydroxyl groups of DEL with acetyl groups are most likely the cause for the observed reductions in water absorption capacity values. Similar trend has been reported earlier [2]. Comparing water sorption capacities of some microcrystalline celluloses with those of ADEL and DEL, the microcrystalline celluloses have lower water sorption capacities [52].

Crude oil uptake values are presented in Fig. 6, as expected, these values increased with increase in sorption time and consistent with findings elsewhere [53]. Moreso, crude oil sorption capacity values for ADEL are always higher than those of DEL, both attaining maximum values of 3.440 g/g for DEL and 4.990 g/g for ADEL after 120 min. Kapok fibres (treated and untreated) [54] and banana fibre (raw and acetylated) [55] had lower crude oil sorption capacities than ADEL and DEL. In contrast, oil sorption capacities of barley straw, wheat straw and oat straw are higher than those of DEL and ADEL as reported by [56]. Considering that oleophilicity is a measure of enhanced non-aqueous sorption property, Fig. 6 demonstrates that ADEL is more oleophilic than DEL. Explanation for this is due to the decrease in hydroxy functionality of DEL by acetylation as ascertained elsewhere [4]. Fig. 6 presents the results for the effect of time on oil sorption. At all times, ADEL absorbed more crude oil than DEL.

### 3.6. Crude oil sorption profiles

#### 3.6.1. Kinetic studies

Understanding the kinetics of crude oil sorption onto DEL and ADEL is vital for practical applications. Particularly, the industrial applications can be feasible if some kinetic parameters are obtained for uses in process designs and scale-up procedures [49]. To anlyse the kinetic profiles for crude oil sorptions by DEL and ADEL, experimental data are fitted to adsorption kinetic models (pseudo-first order, pseudo-second order, intra-particle diffusion, liquid film diffusion and Elovich). In the present study, the pseudo-first order, pseudo-second order, intraparticle diffusion, liquid film diffusion and Elovich kinetic models were applied to investigate the sorption kinetics as shown in equations (23)–(27) respectively [51,57]:

$$\ln(q_e - q_t) = \ln q_e - k_1 t \quad (23)$$

$$\frac{t}{q_t} = \frac{1}{k_2 q_e^2} + \frac{t}{q_e} \quad (24)$$

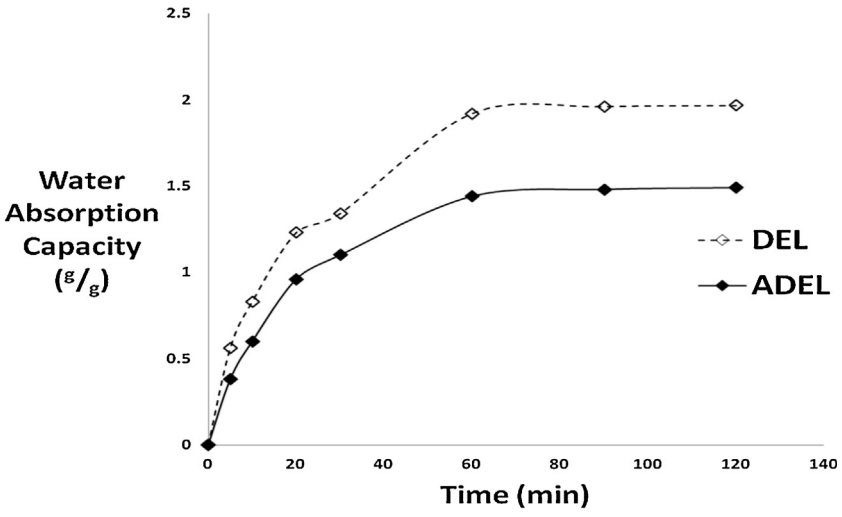


**Fig. 5.** Effect of time on water absorption capacity.

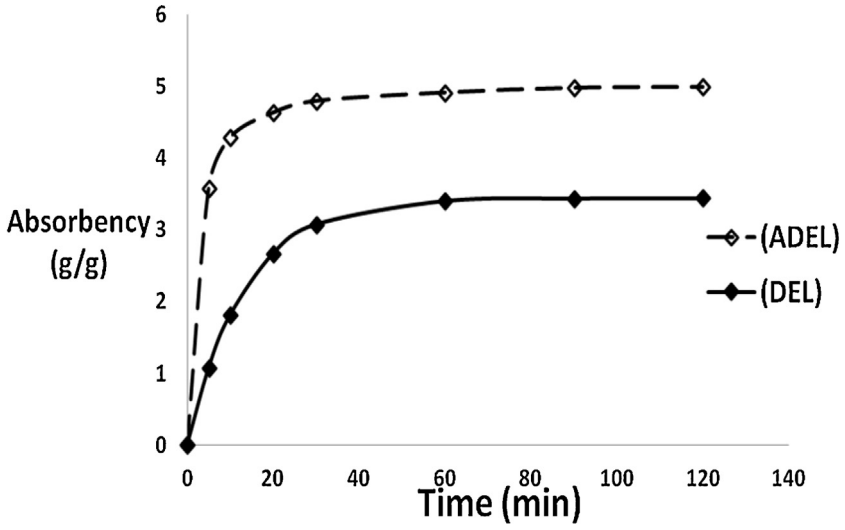


**Fig. 6.** Effect of time on oil sorption capacity.

$$q_t = k_i\sqrt{t} + C \tag{25}$$

$$\ln(1 - F) = -k_{lfd}\cdot t \tag{26}$$

$$q_t = \frac{1}{\beta}\ln(\alpha\beta) + \frac{1}{\beta}\ln t \tag{27}$$

where $k_1$ is the constant of pseudo-first order constant, $k_2$ is the pseudo-second order constant, $k_i$ is the intraparticle diffusion constant, C is a constant (of integration) which gives information about sorption mechanism, $\alpha$ is the initial adsorption rate constant, $\beta$ is related to the extent of surface coverage and activation energy for chemisorption, F is fractional equilibrium attainment, $k_{lfd}$ is the liquid film diffusion constant, and $q_t$ is the amount of dye biosorbed at time t. The determined model parameters and constants are given in Table 4.

**Table 4**
Kinetic parameters.

| Model | ADEL | DEL |
|---|---|---|
| $q_{e,exp}$ (mg/g) | 4990.000 | 3440.000 |
| Pseudo-first order | | |
| $k_1$ ($mg\,g^{-1}min^{-1}$) | 0.0725 | 0.0751 |
| $q_{e,cal}$ (mg/g) | 4793.902 | 3445.416 |
| $R^2$ | 0.6486 | 1.000 |
| Pseudo-second order | | |
| $k_2$ ($gmg^{-1}\,min^{-1}$) | $1.3333 \times 10^{-4}$ | $(5.000 \times 10^{-5})$ |
| $q_{e,cal}$ (mg/g) | 5000 | 3333.33 |
| $R^2$ | 0.9998 | 0.9931 |
| Intraparticle diffusion | | |
| $k_i$ ($mg\,g^{-1}\,min^{-1}$) | 130.600 | 247.870 |
| C | 3782.900 | 1161.000 |
| $R^2$ | 0.6963 | 0.7671 |
| Liquid film diffusion | | |
| $k_{lfd}$ ($min^{-1}$) | 0.0568 | 0.0751 |
| $R^2$ | 0.9222 | 1.000 |
| Elovich | | |
| $\alpha$ (mg/g) | $1.095 \times 10^6$ | 905.475 |
| $\beta$ ($g\,min\,mg^{-1}$) | $2.455 \times 10^{-3}$ | $1.318 \times 10^{-3}$ |
| $R^2$ | 0.8632 | 0.9167 |

Table 4 presents $R^2$ values for the tested kinetic models. $R^2$ values for DEL are: 1.0000 (pseudo-first order), 0.9931 (pseudo-second order), 0.7671 (intra-particle diffusion), 1.0000 (liquid film diffusion) and 0.9167 (Elovich). Fig. 7a shows how the kinetic models compare for experimental. Pseudo-first order and liquid film diffusion kinetic models gave the best fits for crude oil sorption on DEL because they gave the highest $R^2$ value. A value of 1161.0000 as integration constant from intraparticle diffusion plot suggests that not only one sorption mechanism was involved [49]. Oil sorption mechanism which was proposed earlier [58] is in excellent agreement because crude oil removal is most likely due to surface adsorption, absorption within the fibre (major step/process) and interfiber capillary distribution. These therefore support that one mechanism is not enough to account for the crude oil sorption processes. Pseudo-second order kinetic model gave a very good fit but predicted adsorption capacity value of 3333.333 mg/g is wide when compared to experimental adsorption capacity value of 3440 mg/g, therefore very likely implies that chemisorption was not only involved or was not majorly involved during crude oil sorption onto DEL.

For ADEL, $R^2$ values are: 0.6486 (pseudo-first order), 0.9998 (pseudo-second order), 0.6963 (intra-particle diffusion), 0.9222 (liquid film diffusion), and 0.8632 (Elovich). These values are presented in Table 4. The intraparticle diffusion kinetic model gave the smallest $R^2$ value for crude oil sorption on ADEL. Fig. 7b shows how the kinetic models compare with experimental data. Pseudo-second order kinetic model gave the best fit for crude oil sorption on ADEL as Fig. 7b presents. A value of 3782.900 mg/g is large as integration constant from intraparticle diffusion plot and suggests that not only one sorption mechanism was involved during crude oil sorption by ADEL. This high value of integration constant possibly suggests chemisorption was involved in the sorption process [49] and further supported by experimental kinetic data fits presented in Fig. 7b.

### 3.6.2. Equilibrium studies

Graphical plot of solid phase concentration versus liquid phase concentration enables the determination of the equilibrium sorption isotherm. The equilibrium isotherms for the sorption of

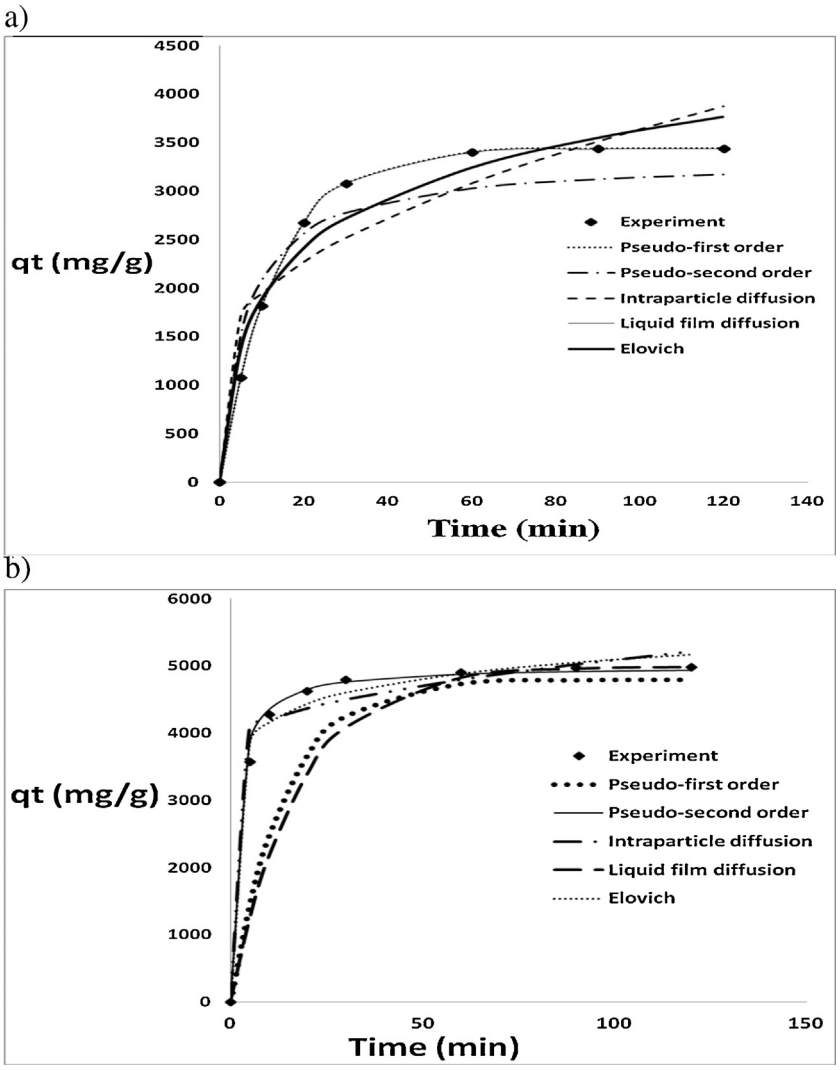


**Fig. 7.** Predicting the kinetic profile of crude oil sorption on DEL (a) and ADEL (b).

crude oil onto DEL have been determined. Many theories abound for explaining sorption equilibrium processes. However, this study presents three isotherm equations as follows [59,60]:

Langmuir

$$\frac{C_e}{q_e} = \frac{1}{q_e b} + \frac{C_e}{q_0} \tag{28}$$

Freundlich

$$\ln q_e = \ln K_F + \frac{1}{n}\ln C_e \tag{29}$$

Temkin

$$q_e = B\ln A + B\ln C_e \tag{30}$$

where $q_e$ (g/g) are the amounts of adsorbed dye per unit weight of sorbents (DEL and ADEL) and $C_e$ (g/L) unadsorbed crude oil concentration in solution at equilibrium, respectively. Langmuir theoretical saturation capacity is represented by $q_0$ (g/g), b is the Langmuir adsorption constant (L/g), $K_F$ is the Freundlich constant, Freundlich heterogeneity constant is represented by "n", and Temkin constants are represented by A and B. Values of the parameters from the isotherms are presented in Table 5.

Langmuir isotherm assumes a monolayer sorption on a surface with non-interacting similar binding sites of uniform energy values. Plot represented by Eq. (28) enabled the calculations of Langmuir constants (b = 0.009109 L/g) and Langmuir theoretical saturation capacity ($q_0$ = 3.8153 g/g) from values of intercept and

**Table 5**
Adsorption isotherm parameters.

| Model | ADEL | DEL |
|---|---|---|
| Langmuir | | |
| $q_o$(g/g) | 5.2411 | 3.8153 |
| b (L/g) | 0.01938 | 0.00911 |
| $R_L$ | 0.094–0.038 | 0.180–0.078 |
| $R^2$ | 0.9985 | 0.9900 |
| Freundlich | | |
| $K_F$(g/g) | 1.0186 | 0.9997 |
| n (g/L) | 4.1649 | 5.5279 |
| $R^2$ | 0.9904 | 0.9902 |
| Temkin | | |
| B (L/g) | 0.7400 | 0.5017 |
| A (g/L) | 1.0520 | 1.0173 |
| $R^2$ | 0.9936 | 0.9877 |

slope respectively, for DEL. The coefficient of determination value, $R^2$, is 0.9900. This value is high and gave a very good prediction of the equilibrium data, as shown in Table 5. There is a Langmuir dimensionless constant ($R_L$), otherwise known as separation factor, known to predict biosorption efficiency and can be determined using the following equation [61]:

$$R_L = \frac{1}{1 + bC_o} \quad (31)$$

where $C_o$ represents the initial crude oil concentration. Calculating values of $R_L$ using different values of $C_o$ gave values of $R_L$ range between $0 < R_L < 1$, reflecting a favorable sorption process [62]. For ADEL, plot of Eq. (28) gave Langmuir constants (b = 0.01938 L/g) and Langmuir theoretical saturation capacity ($q_0$ = 5.2411 g/g) from values of intercept and slope respectively. The value of $q_0$ for ADEL is larger than that obtained for DEL suggesting that ADEL has more saturation capacity. The coefficient of determination value, $R^2$, is 0.9985 for ADEL. This value is high and gave the best prediction of the equilibrium data, as shown in Table 5. Values of $R_L$ calculated using different values of $C_o$ gave $R_L$ values in the range $0 < R_L < 1$, reflecting a favourable sorption process [62]. Calculated $R_L$ range of values are presented in Table 5. $R_L$ values for ADEL are smaller than those of DEL indicating that crude oil sorption was better by ADEL. The modification of DEL by acetylation, to give ADEL, was most likely the reason for the enhanced crude oil sorption. Similar results are reported earlier from our laboratory [2].

Freundlich isotherm assumes a multilayer sorption on a surface with non-similar binding sites of non-uniform energy values. Plot of Eq. (29) enabled the calculations of Freundlich constants ($K_F$ = 0.9997 g/g and n = 5.5279 g/L) from values of intercept and slope respectively, for DEL. The value of $R^2$ is 0.9902. For ADEL, calculations of Freundlich constants from intercept and slope are ($K_F$ = 1.0186 g/g and n = 4.1649 g/L) respectively. The value of $R^2$ is 0.9904. Equilibrium constant value predicted by Freundlich isotherm ($K_F$), has value more than unity, hence, suggests favourable crude oil sorption onto ADEL. DEL has equilibrium constant value predicted by Freundlich isotherm ($K_F$) to be almost unity. Therefore, $K_F$ value for ADEL is higher than for DEL suggesting more favourable sorption process. Freundlich heterogeneity constants for DEL and ADEL are higher than unity suggesting that the crude oil sorption processes were heterogeneous.

The Temkin isotherm is represented by Eq. (30). It assumes a multilayer sorption but differs from the Freundlich mechanism in that the sorbent binding sites possess logarithmic energies. Eq. (30) plot for DEL, enabled the calculations of Temkin constants (B = 0.5017 L/g and A = 1.0173 g/L) from values of slope and intercept respectively and has $R^2$ value of 0.9877. 'A' is Temkin's constant which is equivalent to equilibrium constant [60]. The value is more than unity and predicts favourable crude oil sorption onto DEL. Eq. (30) plot for ADEL, enabled the calculations of Temkin constants (B = 0.7400 L/g and A = 1.0520 g/L) from values of slope and intercept respectively and has $R^2$ value of 0.9936. Temkin's constant, 'A' which is equivalent to equilibrium constant [60], has a value greater than unity suggesting favourable crude oil sorption onto ADEL. Temkin's constant, 'A', has value larger for ADEL than for DEL implying that the crude oil sorption by ADEL was more favourable than by DEL.

Table 5 presents $R^2$ values for the isotherms tested such that the Langmuir isotherm gave the highest value for crude oil sorption by ADEL and the Freundlich isotherm gave the best value for crude oil sorption by DEL.

## 4. Conclusions

Information from the proximate analyses reveal that DEL has long shelf life (moisture content) and good mineral composition (ash level). Therefore, DEL is seemingly not toxic [7], it can be eaten as vegetables by man and ruminants alike. These results suggest therefore that modification of DEL by acetylation and subsequent application in treatment of crude oil polluted water is environmentally safe.

Results of DEL acetylation revealed successful DEL acetylation. Best acetylation conditions are at increased time of acetylation, low acetylation temperature and low amount of catalyst. In agreement with some thermodynamic parameters (heat of acetylation, Gibb's free energy and critical temperature of acetylation), DEL acetylation was effective and can take place under mild or non-severe temperature and ordinary (atmospheric) pressure conditions.

Crude oil sorption kinetic data were best fitted by liquid film diffusion and pseudo-first order kinetic models for DEL. But the pseudo-second order kinetic model best fits crude oil sorption data by ADEL. Langmuir and Freundlich isotherms gave the best fit to the equilibrium crude oil sorption data for ADEL and DEL respectively.

The crude oil and water sorption properties of DEL were reduced and enhanced respectively. In contrast, ADEL had its sorption properties enhanced and reduced respectively for crude oil and water sorption processes. Therefore, ADEL can be deployed as a sorbent for oil spillage treatment. Considering that DEL is an agricultural waste material, it can be easily obtained, abundant, cheap and economical to modify by acetylation, therefore, ADEL is highly recommended for non-aqueous sorption processes.

## Acknowledgement

The authors are thankful to the reviewers for their valuable comments and suggestions that were very helpful and had this work greatly improved.

## References

[1] M.O. Adebajo, R.L. Frost, J.T. Kloprogge, O. Carmody, S. Kokot, Porous materials for oil spill cleanup: a review of synthetic and absorbing properties, J. Porous Mater. 10 (2003) 159–170.
[2] J.O. Nwadiogbu, P.A.C. Okoye, V.I. Ajiwe, N.J.N. Nnaji, Hydrophobic treatment of corn cob by acetylation: kinetics and thermodynamics studies, J. Environ. Chem. Eng. 2 (2014) 1699–1704.
[3] E.T. Nwankwere, C.E. Gimba, J.A. Kagbu, B.K. Nale, Sorption studies of crude oil on acetylated rice husks, Adv. Appl. Sci. Res. 496 (2) (2010) 142–145.
[4] R. Bodirlau, C.A. Teaca, Fourier transform infrared spectroscopy and thermal analysis of lignocellulosic fillers treated with organic anhydride, Rom. J. Phys. 54 (2009) 93–104.
[5] M.D. Teli, S.P. Valia, Acetylation of banana fibre to improve oil absorbency, Carbohydr. Polym. 92 (2013) 328–333.
[6] J. Wanga, Y. Zheng, A. Wang, Superhydrophobic kapok fiber oil-absorbent: preparation and high oil absorbency, Chem. Eng. J. 213 (2012) 1–7.
[7] K.K. Ajibesin, Dacryodes edulis (G. Don) H.J. Lam: a review on its medicinal, phytochemical and economical properties, Res. J. Med. Plant 5 (1) (2011) 32–41.
[8] E.U. Ikhuoria, M. Maliki, Characterization of avocado pear (Persea americana) and African pear (Dacryodes edulis) extracts, Afr. J. Biotechnol. 6 (7) (2007) 950–952.
[9] D.E. Okwu, F.U. Nnamdi, Evaluation of the chemical composition of *Dacryodes Edulis* and *Raphia Hookeri* Mann and Wendl exudates used in herbal medicine in South Eastern Nigeria, Afr. J. Tradit. Complement. Altern. Med. 5 (2) (2008) 194–200.
[10] S.A. Umoren, I.B. Obot, E.E. Ebenso, N. Obi-Egbedi, Studies on the inhibitive effect of exudate gum from Dacroydes edulis on the acid corrosion of aluminium, Portugaliae Electrochim. Acta 26 (2008) 199–209.
[11] E.E. Oguzie, C.K. Enenebeaku, C.O. Akalezi, S.C. Okoro, A.A. Ayuk, E.N. Ejike, Adsorption and corrosion-inhibiting effect of Dacryodis edulis extract on low-carbon-steel corrosion in acidic media, J. Colloid Interface Sci. 349 (2010) 283–292.

[12] T.T. Lim, X. Huang, In situ oil/water separation using hydrophobic-oleophilic fibrous wall: a lab-scale feasible study for groundwater cleanup, J. Hazard. Mater. B137 (2006) 820–826.
[13] J. Idris, G.D. Eyu, A.M. Mansor, Z. Ahmad, C.S. Chukwuekezie, A preliminary study of biodegradable waste as sorbent material for oil-spill cleanup, Sci. World J. (2014). (accessed 19.05.16) http://www.10.1155/2014/638687.
[14] C. Senanurakwarkul, T. Chavarnakul, The study of factors influencing the decision to select the use of oil sorbent in Thailand, Int. J. Res. Manag. Technol. 2 (6) (2012) 603–607.
[15] T.T. Lim, X. Huang, Evaluation of kapok (*Ceiba pentandra* (*L.*) Gaertn,) as a natural hollow hydrophobic-oleophilic fibrous sorbent for oil spill cleanup, Chemosphere 66 (2007) 955–963.
[16] Ch. Teas, S. Kalligeros, F. Zanikos, S. Stournas, E. Lois, G. Anastopoulous, Investigation of the effectiveness of absorbent materials in oil spills clean up, Desalination 140 (2001) 259–264.
[17] H.M. Choi, Needle punched cotton nonwovens and other natural fibers as oil cleanup sorbents, J. Environ. Sci. Health A 31 (6) (1996) 1441–1457.
[18] P.M. Ejikeme, Investigation of the physicochemical properties of microcrystalline cellulose from agricultural wastes 1: orange mesocarp, Cellulose 15 (1) (2008) 141–147.
[19] P. Kaur, S.K. Singh, V. Garg, M. Gulati, Y. Vaidya, Optimization of spray drying process for formulation of solid dispersion containing polypeptide-k powder through quality by design approach, Powder Technol. 284 (2015) 1–11.
[20] M.O. Adebajo, R.L. Frost, Acetylation of raw cotton for oil spill cleanup application: an FTIR and C-13 MAS NMR spectroscopic investigation, Spectrochim. Acta Part A 60 (10) (2004) 2315–2321.
[21] H.H. Sokker, N.M. El-Sawy, M.A. Hassan, B.E. El-Anadouli, Adsorption of crude oil from aqueous solution by hydrogel of chitosan based polyacrylamide prepared by radiation induced graft polymerization, J. Hazard. Mater. 190 (2011) 359–365.
[22] E.I. Unuabonah, K.O. Adebowale, B.I. Olu-Owolabi, L.Z. Yang, L.X. Kong, Adsorption of Pb(II) and Cd(II) from aqueous solutions onto sodium tetraborate-modified kaolinite clay: equilibrium and thermodynamic studies, Hydrometallurgy 93 (2008) 1–9.
[23] C.C. Okaraonye, J.C. Ikewuchi, Nutritional and antinutritional components of pennisetum purpureum (Schumach), Pakistan J. Nutr. 8 (1) (2009) 32–34.
[24] M. Ayub, S. Wahab, Y. Durrani, Effect of water activity ($A_w$) moisture content and total microbial count on the overall quality of bread, Int. J. Agric. Biol. 5 (3) (2003) 274–278.
[25] W.S. Scott, Water relations of food spoilage microorganisms, Adv. Food Res. 7 (1980) 84–127.
[26] H.O. Egharevba, F.O. Kunle, Preliminary phytochemical and proximate analysis of the leaves of Piliostigma thonningii (Schumach.) Milneredhead, Ethnobotanical Leaflets 14 (2010) 570–577.
[27] X.M. Wang, J. Zhang, L.H. Wub, Y.L. Zhao, T. Li, J.Q. Li, Y.Z. Wang, H.G. Liu, A mini-review of chemical composition and nutritional value of edible wild-grown mushroom from China, Food Chem. 151 (2014) 279–285.
[28] A.K. Bledzki, J. Gassan, Composites reinforced with cellulose based fibres, Prog. Polym. Sci. 24 (1999) 221–274.
[29] J.O. Nwadiogbu, V.I.E. Ajiwe, P.A.C. Okoye, Removal of crude oil from aqueous medium by sorption on hydrophobic corncobs: equilibrium and kinetic studies, J. Taibah Univ. Sci. 10 (1) (2016) 56–63.
[30] D. Angelova, I. Uzunovb, S. Uzunova, A. Gigova, L. Minchev, Kinetics of oil and oil products adsorption by carbonized rice husks, Chem. Eng. J. 172 (2011) 306–311.
[31] N. Johae, I. Ahmad, A. Dufresne, Extraction, preparation and characterization of cellulose fibres and nanocrystals from rice husk, Ind. Crops Prod. 37 (1) (2012) 93–99.
[32] H.A. Silverio, W.P.F. Neto, N.O. Dantas, D. Pasquini, Extraction and characterization of cellulose nanocrystals from corncob for application as reinforcing agent in nanocomposites, Ind. Crops Prod. 44 (2013) 427–436.
[33] S. van Santen, Q. deMast, D.W. Swinkels, A.J.A.M. van der Ven, The iron link between malaria and invasive non-typhoid *Salmonella* infections, Trends Parasitol. 29 (2013) 220–227.
[34] A.H. Shanker, Nutritional modulation of malaria morbidity and mortality, J Infect. Dis. 182 (2000) S37–S53.
[35] K.O. Soetan, C.O. Olaiya, O.E. Oyewole, The importance of mineral elements for humans, domestic animals and plants: a review, Afr. J. Food Sci. 4 (2010) 200–222.
[36] C.Y. Aremu, E.I. Udoessien, Chemical estimation of some inorganic elements in selected tropical fruits and vegetables, Food Chem. 37 (1990) 229–234.
[37] T.R. Annunciado, T.H.D. Sydenstricker, S.C. Amico, Experimental investigation of various vegetable fibres as sorbent materials for oil spills, Mar. Pollut. Bull. 50 (2005) 1340–1346.
[38] X.F. Sun, R. Sun, J.X. Sun, Acetylation of rice straw for oil sorption: with or without catalysts, J. Agric. Food Chem. 50 (2002) 6428–6433.
[39] X.F. Sun, R.C. Sun, J.X. Sun, Acetylation of sugarcane bagasse using NBS as a catalyst under mild reaction conditions for the production of oil sorption-active materials, Bioresour. Technol. 95 (2004) 343–350.
[40] R.S. Rengasamy, D. Das, C.P. Karan, Study of oil sorption behavior of filled and structured fiber assemblies made from polypropylene, kapok and milkweed fibers, J. Hazard. Mater. 186 (2011) 526–532.
[41] Y. Luo, V.K. Guda, E.B. Hassan, P.H. Steele, B. Mitchell, F. Yu, Hydrogenation of oxidized distilled bio-oil for the production of gasoline fuel type, Energy Convers. Manag. 112 (2016) 319–327.
[42] G. Ramadoss, K. Muthukumar, Mechanistic study on ultrasound assissted pretreatment of sugarcane bagasse using metal salt with hydrogen peroxide for bioethanol production, Ultrason. Sonochem. 28 (2016) 207–217.
[43] G.C. Xu, J.C. Ding, R.Z. Han, J.J. Dong, Y. Ni, Enhancing cellulose accessibility of corn stover by deep eutetic solvent pretreatment for butanol fermentation, Bioresour. Technol. 203 (2016) 364–369.
[44] M. Kumar, A. Singhal, I.S. Thakur, Comparison of submerged and solid state pretreatment of sugarcane biogasse by *Pandoraea sp.* ISTKB: enzymatic and structural analysis, Bioresour. Technol. 203 (2016) 18–25.
[45] C. Zhao, Q. Shao, Z. Ma, B. Li, X. Zhao, Physical and chemical characterization of corn stalk resulting from hydrogen peroxide presoaking prior to ammonia fiber expansion pretreatment, Ind. Crops Prod. 83 (2016) 86–93.
[46] C.I.K. Diop, H.L. Li, B.J. Xie, J. Shi, Effects of acetic acid/acetic anhydride ratios on the properties of corn starch acetates, Food Chem. 126 (2011) 1662–1669.
[47] D. Chen, A.P. Zhang, C.F. Liu, R.C. Sun, Modification of sugarcane bagasse with acetic anhydride and butyric anhydride in ionic liquid 1-butyl-3-methyl-imidazolium chloride, Bioresoures 7 (3) (2012) 3476–3487.
[48] C.A.S. Hill, D. Jones, G. Strickland, N.S. Cetin, Kinetic and mechanistic aspects of the acetylation of wood with acetic anhydride, Holzforschung 52 (1998) 623–629.
[49] D. Fatih, Dye removal by almond shell residues: Studies on biosorption performance and process design, Mater. Sci. Eng. C 33 (2013) 2821–2826.
[50] N.M. Dowine, R.W. Heath, Basic Statistical Methods, fourth ed., Harper and Row, New York, 1974.
[51] E. Bulut, M. Ozacar, A.I. Sengil, Equilibrium and kinetic data and process design for adsorption of Congo Red onto bentonite, J. Hazard. Mater. 154 (2008) 613–622.
[52] J. Roja, S. Moren, A. Lopez, Assessment of the water sorption properties of several microcrystalline celluloses, J. Pharm. Sci. Res. 3 (7) (2011) 1302–1309.
[53] F.A. Aisien, R.O. Ebewele, F.K. Hymore, Mathematical model ofsorption kinetics of crude oil by rubber particles from scrap tyres, Leonardo J. Sci. 18 (2011) 85–96.
[54] J. Wang, Y. Zheng, A. Wang, Effect of kapok fiber treated with various solvents on oil absorbency, Ind. Crops Prod. 40 (2012) 178–184.
[55] M.D. Teli, S.P. Valia, Acetylation of banana fibre to improve oil absorbency, Carbohydr. Polym. 92 (2013) 328–333.
[56] M.M. Tijani, A. Aqsha, N. Mahinpey, Development of oil-spill sorbent from straw biomass waste: experiments and modelling studies, J. Environ. Manag. 171 (2016) 166–176.
[57] S.R. Taffarel, J. Rubio, On the removal ofMn(II) ions by adsorption onto natural and activated Chilean zeolites, Miner. Eng. 22 (567) (2009) 336–343.
[58] V. Singh, R.J. Kendall, K. Hake, S. Ramkumar, Crude oil sorption by raw cotton, Ind. Eng. Chem. Res. 52 (2013) 6277–6281.
[59] P. Miretzky, C. Munoz, A.C. Chavez, Cd(II) removal from aqueous solution by *Eleocharis acicularis* biomass, equilibrium and kinetic studies, Bioresour. Technol. 101 (2010) 2637–2642.
[60] N.J.N. Nnaji, C.O.B. Okoye, N.O. Obi-Egbedi, M.A. Ezeokonkwo, J.U. Ani, Spectroscopic characterization of red onion skin tannin and it's use as alternative aluminium corrosion inhibitor in hydrochloric acid solutions, Inj. J. Electrochem. Sci. 8 (2013) 1735–1758.
[61] A.G. Ari, S. Celik, Biosorption potential of Orange G dye by modified *Pyracantha coccinea*: batch and dynamic flow system applications, Chem. Engr. J. 226 (2013) 263–270.
[62] S.G. Susmita, G. Krishna, K.G. Bhattacharyya, Adsorption of Ni(II) on clays, J. Colloid Interface Sci. 295 (2006) 21–32.